ELSEVIER

Journal of Organometallic Chemistry 542 (1997) 35–49

Journal of Organometallic Chemistry

Insertion of $GeCl_2$ into group VI transition metal–chlorine bonds: synthesis, spectroscopy and structure of molybdenum and tungsten trichlorogermyl complexes

Alexander C. Filippou *, Johannes G. Winter, Gabriele Kociok-Köhn, Isolde Hinz

Institut für Anorganische und Allgemeine Chemie, Humboldt-Universität zu Berlin, Hessische Str. 1–2, D-10115 Berlin, Germany

Received 18 March 1997; accepted 28 April 1997

Abstract

An efficient method for the synthesis of trichlorogermyl complexes is reported involving the insertion of $GeCl_2$ into the metal–chlorine bond of Group VI transition metal complexes bearing a cyclopentadienyl (Cp) or a pentamethylcyclopentadienyl (Cp*) ligand. This is demonstrated by the reactions of the complexes (η^5-C_5R_5)M(CO)$_3$Cl (**1a–1c**) (**a**: R = H, M = Mo, **b**: R = H, M = W; **c**: R = Me, M = W) and *cis*-CpM(CO)$_2$(L)Cl (**3a**, **5b**) (**3a**: M = Mo, L = PMe_3 **5b**: M = W, L = EtNC) with $GeCl_2$(dioxane), which afford selectively the trichlorogermyl complexes (η^5-C_5R_5)M(CO)$_3$$GeCl_3$ (**2a–2c**) and *cis*-CpM(CO)$_2$(L)$GeCl_3$ (***cis*-4a**, **6b**), respectively. The complex *cis*-CpMo(CO)$_2$(PMe_3)$GeCl_3$ (***cis*-4a**) isomerizes in solution and in solid-state to *trans*-CpMo(CO)$_2$(PMe_3)$GeCl_3$ (***trans*-4a**). The $GeCl_2$-insertion reaction offers a more convenient method for the synthesis of Group VI transition metal trichlorogermyl complexes as shown by a comparison of the syntheses of *cis*-Cp*W(CO)$_2$(EtNC)$GeCl_3$ (**6c**) from *cis*-Cp*W(CO)$_2$(EtNC)Cl (**5c**) and $GeCl_2$(dioxane) or from Na[Cp*W(CO)$_2$(EtNC)] (**7c**) and $GeCl_4$. The crystal structures of the trichlorogermyl complexes **2a**, **2c**, ***trans*-4a** and **6c** are reported. © 1997 Elsevier Science S.A.

Keywords: Germanium; Trichlorogermyl complexes; Molybdenum; Tungsten; Insertion

1. Introduction

Numerous studies have been carried out on germylenes, the germanium analogues of carbenes [1,2]. Most of these compounds are not stable under normal conditions and therefore have been prepared in situ and used as reactive synthons [1]. Stabilisation can be achieved using bulky and π-donor substituents [3]. This leads to compounds, which are stable at ambient temperature and monomeric in solid state [3]. Among the oldest known stable divalent germanium compounds are the dihalides, which have been shown to insert into various σ bonds between main-group elements [1]. In comparison, only few reports have appeared in the literature on insertion reactions of germanium dihalides into σ bonds of transition metals [4]. This has prompted the following work dealing with the insertion of $GeCl_2$ into the M–Cl bond of various molybdenum and tungsten complexes bearing a cyclopentadienyl or pentamethylcyclopentadienyl ligand.

2. Results and discussion

Starting materials for reactions described below were the chloro complexes (η^5-C_5R_5)M(CO)$_3$Cl (**1a–1c**) (**a**: R = H, M = Mo, **b**: R = H, M = W; **c**: R = Me, M = W). These were obtained in 80–90% yield by the oxidation of the metallates M'[(η^5-C_5R_5)M(CO)$_3$] (M' = Na, K) with one equivalent of $PhICl_2$. The metallates were prepared in situ upon heating the metal hexacarbonyls with NaCp or KCp* in 1,2-dimethoxyethane (DME) (Scheme 1). This one-pot procedure for the synthesis of the chloro complexes **1a–1c** is a faster and higher-yield method than the previously reported methods involving either protonation of the metallates M'[(η^5-C_5R_5)M(CO)$_3$] to give the hydrides (η^5-C_5R_5)M(CO)$_3$H followed by their chlorination with CCl_4 [5], or oxidation of the metallates with ferric sulphate to afford the complexes (η^5-C_5R_5)$_2$M$_2$(CO)$_6$ [6] followed by their irradiation in CCl_4 [7].

When the chloro complexes **1a–1c** were treated with one equivalent of $GeCl_2$(dioxane) in CH_2Cl_2 at −78°C and subsequently the reaction solutions were warmed to

* Corresponding author.

0022-328X/97/$17.00 © 1997 Elsevier Science S.A. All rights reserved.
PII S0022-328X(97)00284-2

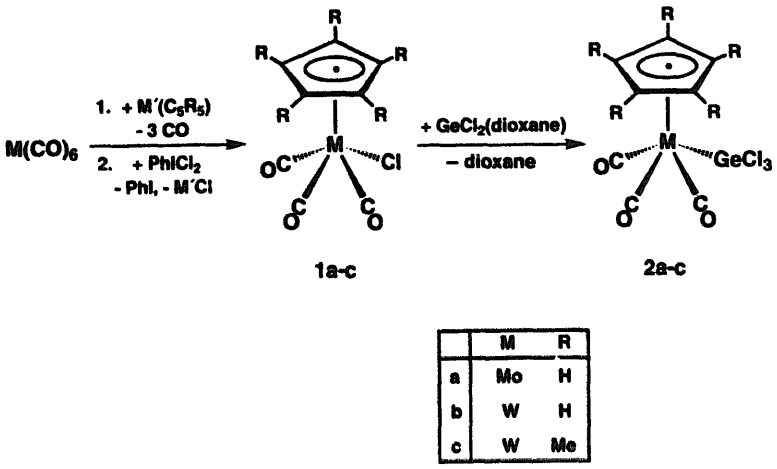

Scheme 1.

room temperature, a selective insertion reaction of $GeCl_2$ into the M–Cl bond of **1a–1c** occurred to give the trichlorogermyl complexes $(\eta^5\text{-}C_5R_5)M(CO)_3GeCl_3$ (**2a–2c**) (Scheme 1). These were isolated as yellow, thermoresistant, air-stable, microcrystalline solids in 97%, 96% and 80% yields, respectively. They are soluble in CH_2Cl_2 and THF, but sparingly soluble in n-pentane and melt at 129°C, 154°C and 160°C, respectively.

Complexes **2a** and **2b** have been previously obtained from **1a** and **1b** and $HGeCl_3$ in diethylether [8]. This reaction presumably occurs also via the insertion of $GeCl_2$ into the M–Cl bond of **1a** and **1b**, $GeCl_2$ being generated in situ from $HGeCl_3$ in diethylether [9]. The trichlorogermyl complexes **2a–2c** are related to the earlier reported trifluorogermyl complex $CpMo(CO)_3GeF_3$, which was prepared from **2a** and $AgBF_4$ [10], the tribromogermyl complex $CpMo(CO)_3GeBr_3$, which was obtained as by-product of the attempted insertion reaction of $GeBr_2$ into the Mo–Mo bond of $Cp_2Mo_2(CO)_6$ [11], and the organogermanium complexes $CpM(CO)_3GeR_3$ (M = Cr, Mo, W; R = alkyl, aryl), which were prepared either by salt elimination from $Na[CpM(CO)_3]$ and R_3GeX (X = Cl, Br) [12], by dimethylamine elimination from $CpM(CO)_3H$ and Me_3GeNMe_2 [13] or by oxidative addition of $CpGeMe_3$ to *fac*-$M(CO)_3(MeCN)_3$ [14].

The solution IR spectra of the complexes **2a–2c** exhibit three ν(CO) absorptions as expected on the basis of group theory for a $M(CO)_3$ fragment of local C_s-symmetry in a 'four-legged piano-stool' complex of the type $(\eta^5\text{-}C_5R_5)M(CO)_3X$ (R = H, Me; M = Cr, Mo, W; X = neutral, one-electron donor ligand) (Table 1) [15].

In addition, the ^{1}H-NMR spectra of **2a–2c** display only one singlet resonance for the protons of the Cp or Cp* ligand (Table 2), and the ^{13}C-NMR spectra show two carbonyl-carbon resonances in an approximate ratio of 2/1 (Table 3). Both carbonyl-carbon resonances appear at higher field than those of the corresponding chloro complexes **1a–1c** indicating in full agreement

Table 1
ν(C ≡ NEt), and ν(CO) absorptions of the complexes **1a–7c** in cm^{-1}; solvents: CH_2Cl_2 (a), THF (b)

Complex	ν(C ≡ NEt)	ν(CO)	Solvent
$CpMo(CO)_3Cl$ (**1a**)	–	2056s, 1977vs, 1964sh	a
		2052s, 1973vs, 1956s	b
$CpW(CO)_3Cl$ (**1b**)	–	2048s, 1958vs	a
		2043s, 1953vs	b
$Cp^*W(CO)_3Cl$ (**1c**)	–	2032s, 1942vs, 1930sh	a
$CpMo(CO)_3GeCl_3$ (**2a**)	–	2051s, 1988m, 1965vs	a
$CpW(CO)_3GeCl_3$ (**2b**)	–	2046s, 1975m, 1954vs	a
$Cp^*W(CO)_3GeCl_3$ (**2c**)	–	2033s, 1959sh, 1946vs	a
cis-$CpMo(CO)_2(PMe_3)Cl$ (**3a**)	–	1966vs, 1864s	a
trans-$[CpMo(CO)_2(PMe_3)_2]Cl$ (**3a'**)	–	1961s, 1880vs	a
cis-$CpMo(CO)_2(PMe_3)GeCl_3$ (*cis*-**4a**)	–	1976vs, 1907s	a
trans-$CpMo(CO)_2(PMe_3)GeCl_3$ (*trans*-**4a**)	–	1965m, 1891s	a
cis-$CpW(CO)_2(EtNC)Cl$ (**5b**)	2172s	1967vs, 1888s	a
cis-$Cp^*W(CO)_2(EtNC)Cl$ (**5c**)	2161m	1947vs, 1868s	a
cis-$CpW(CO)_2(EtNC)GeCl_3$ (**6b**)	2166m	1984vs, 1916s	a
cis-$Cp^*W(CO)_2(EtNC)GeCl_3$ (**6c**)	2159m	1970vs, 1904s	a
$Na[Cp^*W(CO)_2(EtNC)]$ (**7c**)	1855s	1749vs, 1690vs	b

Table 2
^{1}H-NMR and ^{31}P-NMR data of the complexes **1a–6c**; relative intensities and multiplicities in parentheses, coupling constants in Hz

Complex	CH_3CH_2NC	$P(CH_3)_3$	C_5Me_5	CH_3CH_2NC	C_5H_5	δ_P	Solvent; temp. (°C)
1a	–	–	–	–	4.55 (5, s)	–	C_6D_6; +20°C
1c	–	–	1.52 (15, s)	–	–	–	C_6D_6; +20°C
2a	–	–	–	–	5.67 (5, s)	–	CD_2Cl_2; +20°C
2b	–	–	–	–	5.77 (5, s)	–	CD_2Cl_2; +20°C
2c	–	–	2.22 (15, s)	–	–	–	$CDCl_3$; +20°C
3a	–	1.10 (9, d) ^2J(PH) = 9.7	–	–	4.74 (5, s)	10.6	C_6D_6; +20°C
3a'	–	1.79 (18, m)	–	–	5.56 (5, s)	18.2	CD_2Cl_2; +20°C
***cis*-4a**	–	1.65 (9, d) ^2J(PH) = 9.7	–	–	5.41 (5, s)	6.1	CD_2Cl_2; −40°C
***cis*-4a**	–	1.72 (9, d) ^2J(PH) = 9.7	–	–	5.42 (5, s)	4.8	CD_2Cl_2; +20°C
***trans*-4a**	–	1.68 (9, d) ^2J(PH) = 9.9	–	–	5.43 (5, s)	19.6	CD_2Cl_2; +20°C
5b	0.60 (3, t) ^3J(HH) = 7.2	–	–	2.89 (2, q) ^3J(HH) = 7.2	4.99 (5, s)	–	C_6D_6; +20°C
5c	0.56 (3, t) ^3J(HH) = 7.2	–	1.77 (15, s)	2.79 (2, q) ^3J(HH) = 7.2	–	–	C_6D_6; +20°C
5c	1.43 (3, t) ^3J(HH) = 7.2	–	1.98 (15, s)	4.03 (2, q) ^3J(HH) = 7.2	–	–	CD_2Cl_2; +20°C
6b	1.46 (3, t) ^3J(HH) = 7.3	–	–	4.03 (2, q) ^3J(HH) = 7.3	5.61 (5, s)	–	CD_2Cl_2; +20°C
6c	1.47 (3, t) ^3J(HH) = 7.3	–	2.15 (15, s)	4.05 (2, q) ^3J(HH) = 7.3	–	–	CD_2Cl_2; +20°C

with the IR spectra, that insertion of $GeCl_2$ into the M–Cl bond of **1a–1c** reduces the electron density at the metal center and weakens thereby the metal(dπ)–CO(π *) back bonding [16].

The molecular structures of the complexes **2a** and **2c** were determined by single-crystal X-ray diffraction studies. Suitable single crystals were obtained after slow evaporation of a CH_2Cl_2 solution of **2a** and **2c** at room temperature. A ZORTEP drawing of a single molecule of **2a** and one of the two molecules of **2c** in the asymmetric unit are shown in Fig. 1 and Fig. 2, respectively. Selected bond lengths and angles of **2a** and **2c** are given in Tables 4 and 5, respectively. For **2c** the discussion is based on the average values of the bond lengths and angles of the two molecules in the asymmetric unit.

The coordination geometry around the molybdenum atom in **2a** and the tungsten atom in **2c** can be described as square–pyramidal with the Cp(Cp*) ligand occupying one coordination site at the apex of the pyramid.

Table 3
^{13}C-NMR data of the complexes **1a–6c**; coupling constants in Hz

Complex	C_5Me_5	CH_3CH_2NC	$P(CH_3)_3$	CH_3CH_2NC	C_5H_5; C_5Me_5	CH_3CH_2NC	CO	Solvent; temp. (°C)
1a	–	–	–	–	95.4		225.0; 243.1	C_6D_6; +20°C
1c	10.3	–	–	–	106.3	–	221.1 ^1J(WC) = 154.2; 237.3	C_6D_6; +20°C
2a	–	–	–	–	93.8	–	222.7; 226.4	CD_2Cl_2; +20°C
2b	–	–	–	–	92.4	–	212.2 ^1J(WC) = 141.8; 213.8	CD_2Cl_2; +20°C
2c	10.8	–	–	–	105.7	–	216.3; 217.8	$CDCl_3$; +20°C
3a	–	–	16.7 (d) ^1J(PC) = 31.1	–	93.7	–	244.3 (d) ^2J(PC) = 6.4; 259.3 (d) ^2J(PC) = 32.1	C_6D_6; +20°C
3a'	–	–	20.9 (m)	–	93.0	–	233.4 (t) ^2J(PC) = 27.3	CD_2Cl_2; +20°C
***cis*-4a**	–	–	21.2 (d) ^1J(PC) = 32.1	–	91.7	–	237.3; 238.7 (d) ^2J(PC) = 30.0	CD_2Cl_2; −70°C
***trans*-4a**	–	–	20.8 (d) ^1J(PC) = 33.7	–	92.1	–	231.4 ^2J(PC) = 27.1	CD_2Cl_2; +20°C
5b	–	15.2	–	40.1	92.9	150.6	232.9; 245.9	C_6D_6; +20°C
5	10.8	15.6	–	39.9	104.7	–	237.6; 250.2	C_6C_6; +20°C
5c	10.8	16.3	–	41.1	105.2	155.9	239.9; 248.7	CD_2Cl_2; +20°C
6b	–	14.9	–	42.1	91.0	142.5	222.5; 224.5	CD_2Cl_2; +20°C
6c	11.2	15.4	–	42.1	104.5	148.9	225.8; 229.5	CD_2Cl_2; +20°C

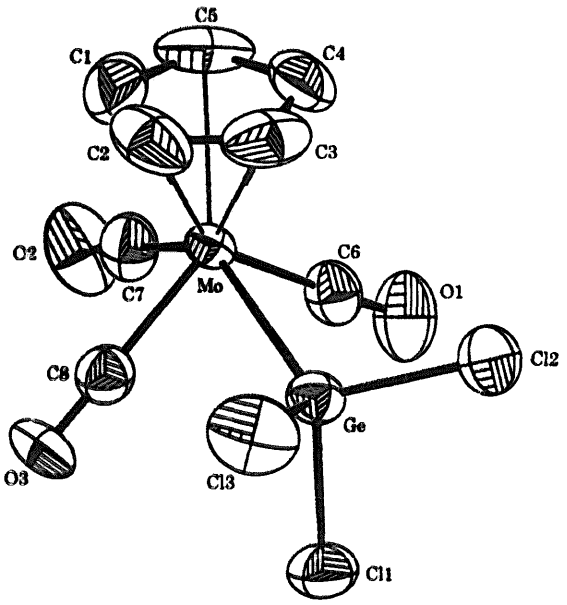

Fig. 1. ZORTEP plot of the structure of **2a** with thermal ellipsoids drawn at the 50% probability level.

This coordination geometry has been observed for a variety of 'four-legged piano-stool' complexes of the type $(\eta^5\text{-}C_5R_5)M(CO)_3X$ (R = H, Me; M = Mo, W; X = one-electron donor ligand) [17]. The basal plane of the pyramid defined by the carbonyl-carbon atoms and the germanium atom is essentially parallel to the Cp (Cp*) ring plane, the dihedral angle between the least square planes being 1.7° in **2a** and 4.6° in **2c**. The Mo–C(ring) bond lengths of **2a** range from 229.0(10) to

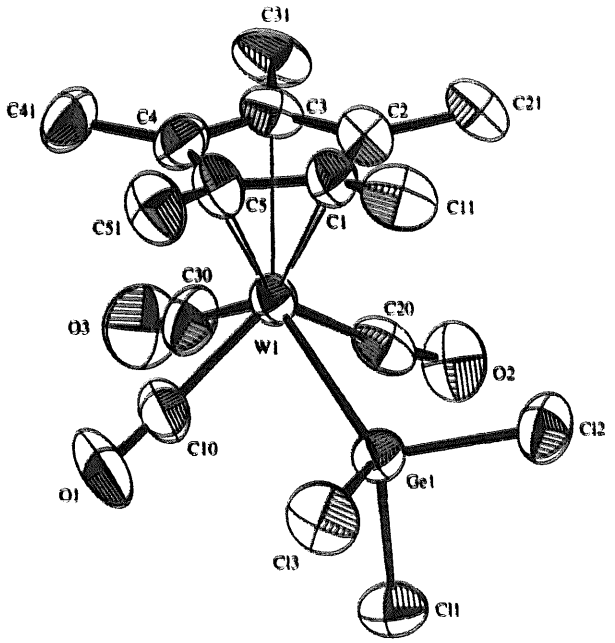

Fig. 2. ZORTEP plot of the structure of one of the two molecules of **2c** in the crystallographic asymmetric unit. Thermal ellipsoids are drawn at the 50% probability level. The second molecule contains the atoms W2, Ge2, Cl4 to Cl6, C6 to C10, C40, C50, C60, C61, C71, C81, C91, C101 and O4 to O6.

Table 4
Selected bond lengths (pm) and bond angles (°) with estimated standard deviations for **2a**

Mo–C(1)	229.0(10)	C(6)–Mo–C(7)	80.0(4)
Mo–C(2)	232.4(10)	C(6)–Mo–C(8)	108.9(3)
Mo–C(3)	232.4(9)	C(6)–Mo–Ge	75.2(2)
Mo–C(4)	233.1(9)	C(7)–Mo–C(8)	77.3(3)
Mo–C(5)	230.8(9)	C(7)–Mo–Ge	132.8(3)
Mo–C(6)	198.8(9)	C(8)–Mo–Ge	73.8(2)
Mo–C(7)	201.0(9)	Mo–Ge–Cl(1)	119.04(8)
Mo–C(8)	199.5(9)	Mo–Ge–Cl(2)	115.30(8)
Mo–Ge	254.55(10)	Mo–Ge–Cl(3)	115.72(9)
Ge–Cl(1)	217.6(2)	Cl(1)–Ge–Cl(2)	102.51(11)
Ge–Cl(2)	217.3(2)	Cl(1)–Ge–Cl(3)	100.05(12)
Ge–Cl(3)	218.0(3)	Cl(2)–Ge–Cl(3)	101.55(12)

233.1(9) pm and the W–C(ring) bond lengths of **2c** from 227(2) to 237.5(13) pm, the average values of 231.5 pm (**2a**) and 232.6 pm (**2c**) being close to those of other Cp- and Cp*-substituted Mo^{II} and W^{II} complexes [17]. The *cis* and *trans* OC–M–CO and OC–M–$GeCl_3$ angles of **2a** and **2c** are within the range found for other 'four-legged piano-stool' complexes of the type $(\eta^5\text{-}C_5R_5)M(CO)_3X$ (R = H, Me; M = Mo, W; X = one-electron donor ligand) [17]. The metal–carbonyl groups are approximately linear, the M–C–O bond angles ranging in **2a** from 177.4(8) to 178.4(8)° and in **2c** from 171.9(12) to 178(2)°. The Mo–CO bond lengths of **2a** are found between 198.8(9) and 201.0(9) pm and the W–CO bond lengths of **2c** between 196(2) and 203(2) pm. They have an average value of 199.8 pm (**2a**) and 199.5 pm (**2c**), which is similar to that of $CpMo(CO)_3Cl$ [$(Mo\text{–}C_{CO})_{av}$ = 199.3 pm] and $CpW(CO)_3Cl$ [$(W\text{–}C_{CO})_{av}$ = 199.8 pm], respectively [18].

The major focus of interest is on the structural features of the trichlorogermyl ligand. The Mo–Ge bond of **2a** is with 254.55(10) pm shorter than the Mo–Ge single bond of the triphenylgermyl complexes $Cp(CO)_2Mo(GePh_3)[C(OEt)Ph]$ [Mo–Ge = 265.8(2) pm] [19] and $Cp(\eta^3\text{-}C_6H_{11})(NO)Mo(GePh_3)$ [Mo–Ge = 260.4(2) pm] [20], and is as expected longer than the Mo–Ge triple bond of $Cp(CO)_2Mo{\equiv}GeC_6H_3\text{-}2,6\text{-}Mes_2$) [Mo–Ge = 227.1(1) pm] [21]. The W–Ge bond

Table 5
Selected bond lengths (pm) and bond angles (°) with estimated standard deviations for **2c**

W(1)–C(1)	237.4(13)	C(20)–W(1)–C(30)	77.2(6)
W(1)–C(2)	234.8(14)	C(10)–W(1)–C(20)	118.6(7)
W(1)–C(3)	230.3(14)	C(20)–W(1)–Ge(1)	73.7(4)
W(1)–C(4)	229.1(14)	C(10)–W(1)–C(30)	78.0(8)
W(1)–C(5)	230.3(13)	C(30)–W(1)–Ge(1)	122.7(5)
W(1)–C(10)	203(2)	C(10)–W(1)–Ge(1)	74.6(5)
W(1)–C(20)	200(2)	W(1)–Ge(1)–Cl(1)	116.33(13)
W(1)–C(30)	200(2)	W(1)–Ge(1)–Cl(2)	118.57(14)
W(1)–Ge(1)	256.3(2)	W(1)–Ge(1)–Cl(3)	118.1(2)
Ge(1)–Cl(1)	218.8(4)	Cl(1)–Ge(1)–Cl(2)	100.0(2)
Ge(1)–Cl(2)	218.1(4)	Cl(1)–Ge(1)–Cl(3)	100.7(2)
Ge(1)–Cl(3)	218.1(4)	Cl(2)–Ge(1)–Cl(3)	99.9(2)

of **2c** is with 256.2 pm slightly longer than that of the W^{IV} germyl complex $Cp_2W(SiMe_3)(GeMe_2Cl)$ [W–Ge = 254.2(1) pm] [22]. The three Ge–Cl bonds of **2a** and **2c** are similar with an average value of 217.6 and 217.9 pm, respectively. They are longer than the Ge–Cl bonds of $GeCl_4$ [$(Ge–Cl)_{av.}$ = 211.3(3) pm] [23], $HGeCl_3$ [$(Ge–Cl)_{av.}$ = 211.8(1) pm] [24], $MeGeCl_3$ [$(Ge–Cl)_{av.}$ = 213.2(4) pm] [25] and $(C_6Cl_5)_3GeCl$ [Ge–Cl = 215.8(2) pm] [26], indicating along with the short M–Ge bond of **2a** and **2c** a hyperconjugation between the metal carbonyl fragment and the trichlorogermyl ligand, which results from $M(d\pi)$–$(Ge–Cl)(\sigma *)$ back bonding. The tetrahedral environment of the germanium atom is in both compounds considerably distorted. Thus, the Cl–Ge–Cl bond angles of **2a** and **2c** are smaller than that of an ideal tetrahedron ranging from 100.05(12) to 102.51(11)° and 99.9(2) to 100.7(2)°, respectively. Consequently, the M–Ge–Cl bond angles are larger than that of an ideal tetrahedron ranging in **2a** from 115.30(8) to 119.04(8)° and in **2c** from 116.33(13) to 118.57(14)°. This distortion results from the larger steric demand of the $(C_5R_5)M(CO)_3$ group and the difference in polarity of the M–Ge and the Ge–Cl bonds [27].

Next we wanted to find out whether the insertion of $GeCl_2$ into a M–Cl bond offers a valuable method also for the synthesis of more electron-rich molybdenum and tungsten complexes. For this purpose we have prepared some CO substitution products of **1a**–**1c** and tested their reactivity towards $GeCl_2$(dioxane).

Treatment of **1a** with PMe_3 in THF at room temperature afforded the desired CO-substitution product *cis*-$CpMo(CO)_2(PMe_3)Cl$ (**3a**) (Eq. (1)). This was isolated in 45% yield as an orange-red, microcrystalline solid, which is soluble in CH_2Cl_2, THF and Et_2O, but sparingly soluble in pentane and decomposes, at 156°C when heated in a sealed capillary under argon.

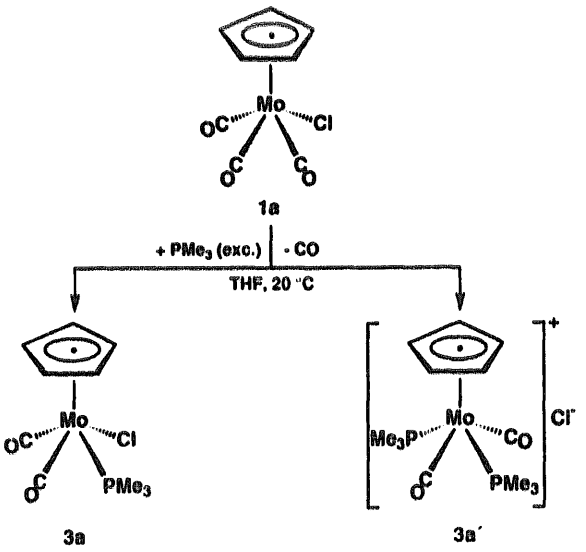

(1)

IR monitoring of the reaction of **1a** with PMe_3 revealed the formation of a second product, which was easily separated from **3a** due to its insolubility in Et_2O and isolated as a yellow solid in 35% yield. This product was characterized by IR, NMR spectroscopy and elemental analysis to be the ionic complex *trans*-$[CpMo(CO)_2(PMe_3)_2]Cl$ (**3a′**) (Eq. (1)). Complex **3a′** is soluble in CH_2Cl_2, moderate soluble in THF, but insoluble in pentane and starts decomposing, when heated in a sealed capillary under argon, at 203°C. IR spectroscopic investigation of a sample of **3a′**, after it has been heated to 210°C, revealed the formation of *trans*-$CpMo(CO)(PMe_3)_2Cl$ as the only decomposition product. This complex was independently prepared by the reduction of $CpMo(CO)(PMe_3)Cl_3$ with two equivalents of Na/Hg in the presence of PMe_3 and was fully characterized [28].

The solution IR spectra of **3a** and **3a′** show two ν(CO) absorption bands (Table 1). For **3a** the higher energy absorption of the symmetric ν(CO) vibration is more intense than the lower energy absorption of the antisymmetric ν(CO) vibration, indicating the presence of the *cis*-isomer [29]. In contrast, the higher energy ν(CO) absorption of **3a′** is less intense than the lower energy ν(CO) absorption, suggesting in agreement with the NMR spectroscopic data the presence of the *trans*-isomer [29]. The angle 2θ between the two CO ligands has been calculated to be 87.7° in **3a** and 105.7° in **3a′** using the relationship $I_a/I_s = \tan^2\theta$, where I_a and I_s are the intensities of the absorptions due to the antisymmetric and symmetric C–O stretching modes [29]. For **3a′** the calculated OC–Mo–CO angle corresponds well to that found in the crystal structure of the complex $[CpMo(CO)_2(PMe_3)_2][CpMo(CO)_3]$ [OC–Mo–CO = 106.9°] [30]. The $^{13}C\{^1H\}$-NMR spectrum of **3a** displays two equally intense resonances for the inequivalent carbonyl ligands at δ 244.3 and 259.3, indicating in agreement with the IR data the presence of the *cis*-isomer. Both resonances appear as doublets due to ^{13}C–^{31}P coupling (Table 3). In comparison, the $^{13}C\{^1H\}$-NMR spectrum of **3a′** shows one resonance for the two equivalent carbonyl ligands at δ 233.4, which appears as a triplet due to ^{13}C–^{31}P coupling with the two equivalent PMe_3 ligands [$^2J(PC)$ = 27.3 Hz] (Table 3). The lower field carbonyl–carbon resonance of **3a** showing the larger splitting is assigned to the CO ligand in *cis* position relative to the PMe_3 ligand. This assignment is based on the size of the $^2J(PC)$ coupling constant [$^2J(PC)$ = 32.1 Hz], which is similar to that of the carbonyl ligands of **3a′** (Table 3) [31]. The $^{31}P\{^1H\}$-NMR spectrum of **3a′** displays one singlet resonance for the two equivalent PMe_3 ligands at δ 18.2 showing unequivocally the *trans* geometry of this compound (Table 2).

A similar reaction to that of **1a** with PMe_3 has been previously reported by Fischer et al. He found that

complex **1b** reacts with PEt_3 in benzene at 80°C to give a mixture of *cis*-$CpW(CO)_2(PEt_3)Cl$ and *trans*-$[CpW(CO)_2(PEt_3)_2]Cl$ [32]. Substitution of carbon monoxide or the halide ligand in the complexes $CpM(CO)_3X$ (M = Cr, Mo, W; X = Cl, Br, I) has been accomplished also with a variety of other neutral donor ligands and the nature of the products of the thermal substitution reactions has been shown to depend upon the basicity and the π-acceptor ability of the entering ligand, the particular halide and the metal center [33]. The cation *trans*-$[CpMo(CO)_2(PMe_3)_2]^+$ has been isolated previously as $[CpMo(CO)_3]^-$ salt from the disproportionation reaction of $Cp_2Mo_2(CO)_6$ with PMe_3, and its crystal structure has been determined [30].

Treatment of **3a** with one equivalent of $GeCl_2$(dioxane) in CH_2Cl_2 at −78°C and subsequent warming of the reaction solution to ambient temperature afforded fast and selectively the insertion product *cis*-$CpMo(CO)_2(PMe_3)GeCl_3$ (***cis*-4a**) (Eq. (2)).

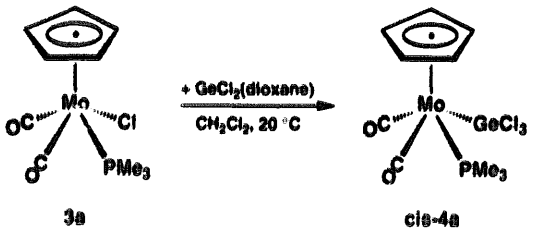

(2)

Evidence for the clean conversion of **3a** to ***cis*-4a** was given by the IR spectra of the reaction solutions, which showed that the ν(CO) absorptions of the starting material at 1966 and 1864 cm^{-1} had been replaced at the end of the reaction by those of the product at 1976 and 1907 cm^{-1}. After evaporation of the solvent and washing of the residue with Et_2O/pentane (1/1), complex ***cis*-4a** was isolated as a yellow, microcrystalline solid in 91% yield. It is soluble in CH_2Cl_2, sparingly soluble in Et_2O, but insoluble in pentane and isomerizes in solution to the *trans*-isomer ***trans*-4a** (Eq. (3)).

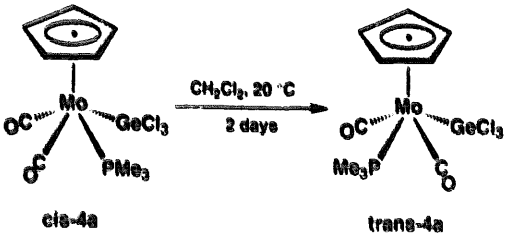

(3)

Isomerization in CH_2Cl_2 at room temperature was found by IR and ^{1}H-NMR spectroscopy to be complete after 2 days. This allowed also the isolation of the *trans*-isomer ***trans*-4a** as a yellow, microcrystalline solid, which melts at 232°C and has similar solubility properties to the *cis*-isomer. Isomerization of the *cis*- to the *trans*-isomer occurs also in the solid state. Thus, when a sample of the *cis*-isomer was sealed into a capillary tube under argon and was heated to 226°C until it melted, the IR spectrum of the cooled melt in CH_2Cl_2 revealed the exclusive formation of the *trans*-isomer.

The identity of the isomers ***cis*-4a** and ***trans*-4a** was proven by spectroscopic means. Thus, two ν(CO) absorption bands are observed in the IR spectra of both isomers (Table 1). For the *cis*-isomer the higher frequency (symmetric) CO stretching vibration gives rise to a more intense absorption than the lower frequency (antisymmetric) CO stretching vibration, whereas the opposite is true for the *trans*-isomer (see also discussion of the IR spectra of **3a** and **3a'**) [29].

The ν(CO) absorptions of ***cis*-4a** appear at higher wavenumbers than those of the chloro complex *cis*-$CpMo(CO)_2(PMe_3)Cl$ (**3a**) indicating in full agreement with the ^{13}C-NMR spectra, that insertion of $GeCl_2$ into the Mo–Cl bond of **3a** reduces the electron density at the metal center and weakens thereby the metal(dπ)–CO(π *) back bonding. The ^{31}P{^{1}H}-NMR spectra of ***cis*-4a** and ***trans*-4a** in CD_2Cl_2 at 20°C display a singlet resonance at δ 4.8 and 19.6, respectively, and both isomers exhibit in the ^{1}H-NMR spectra a doublet resonance for the PMe_3 protons and a singlet resonance for the cyclopentadienyl ring protons (Table 2). In the ^{13}C{^{1}H}-NMR spectrum of ***cis*-4a** two carbon resonances for the nonequivalent carbonyl ligands at δ 237.3 and 238.7 are observed, with the latter resonance appearing as a doublet due to ^{13}C–^{31}P coupling. This resonance can be assigned to the carbonyl ligand, which occupies a *cis*-position relative to the PMe_3 ligand. This assignment is based on the size of the ^2J(PC) coupling constant (30.0 Hz), which is similar to that of the equivalent carbonyl ligands of the trans- isomer [^2J(PC) = 27.1 Hz] (see also discussion of the ^{13}C{^{1}H}-NMR spectra of **3a** and **3a'**) (Table 3) [31]. Both carbonyl-carbon resonances of ***cis*-4a** appear at higher field than those of *cis*-$CpMo(CO)_2(PMe_3)Cl$ (**3a**) indicating in good agreement with the IR spectra a weaker M(dπ)–CO(π *) back bonding in ***cis*-4a** [16,31].

The solid-state structure of the *trans*-isomer was determined by a single-crystal X-ray diffraction study. Suitable single crystals were obtained after slow evaporation of a CH_2Cl_2 solution of ***trans*-4a** at room temperature. A ZORTEP drawing of one of the two molecules of ***trans*-4a** in the asymmetric unit with the atom-labeling scheme adopted is shown in Fig. 3. Selected bond lengths and angles of ***trans*-4a** are listed in Table 6. The discussion of the structure of ***trans*-4a** presented below is based on the average values of the

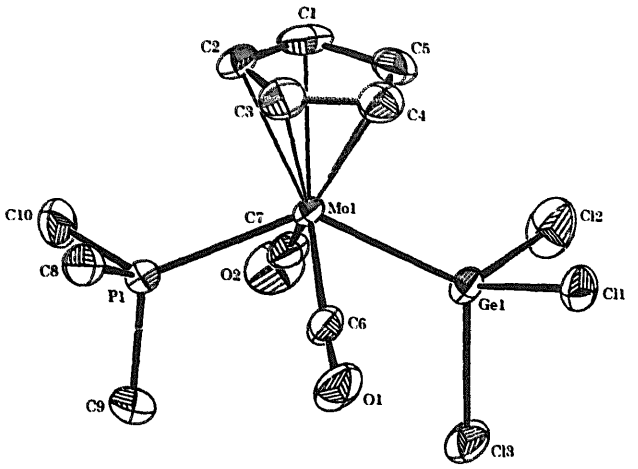

Fig. 3. ZORTEP plot of the structure of one of the two molecules of ***trans*-4a** in the crystallographic asymmetric unit. Thermal ellipsoids are drawn at the 30% probability level. The second molecule contains the atoms Mo2, Ge2, P2, Cl4 to Cl6, C11 to C20, O3 and O4.

bond lengths and angles of the two molecules in the asymmetric unit.

Complex ***trans*-4a** shows the expected square-pyramidal coordination geometry of a 'four-legged piano-stool' complex with a *trans* disposition of the trichlorogermyl and the trimethylphosphane ligand. The Mo–C(ring) bond lengths range from 229.4(6) to 236.0(6) pm and have an average value of 231.8 pm, which is very close to that of **2a** [$(Mo–C_{ring})_{av.}$ = 231.5 pm]. The *trans* OC–Mo–CO and Me_3P–Mo–$GeCl_3$ bond angles of ***trans*-4a** are similar to the *trans* OC–Mo–CO and *trans* OC–Mo–$GeCl_3$ bond angles of **2a** and are in the range also found for other 'four-legged piano-stool' complexes of the type *trans*-CpM(CO)$_2$LX (L = two-electron donor ligand; X = one-electron donor ligand) [34]. The molybdenum–carbonyl groups are approximately linear, the Mo–C–O bond angles ranging from 174.5(6) to 176.7(5)°. The Mo–CO bonds of ***trans*-4a** are shorter than those of **2a** having an average length of 197.6 pm [**2a**: $(Mo–CO)_{av.}$ = 199.8 pm]. This indicates in good agreement with the IR and ^{13}C-NMR spectra a stronger M(dπ)–CO(π*) back bonding in ***trans*-4a** than in **2a**. A comparison of the structural parameters of the trichlorogermyl ligand in **2a** and in ***trans*-4a** reveals that substitution of the carbonyl by the PMe_3 ligand results in a shortening of the Mo–Ge bond [**2a**: Mo–Ge = 254.55(10) pm; ***trans*-4a**: $(Mo–Ge)_{av.}$ = 250.57 pm], an elongation of the Ge–Cl bonds [**2a**: $(Ge–Cl)_{av.}$ = 217.6 pm; ***trans*-4a**: $(Ge–Cl)_{av.}$ = 219.3 pm] and a larger distortion of the tetrahedral environment of the germanium atom. Thus, the Cl–Ge–Cl bond angles of ***trans*-4a** are even more acute than those of **2a** having an average value of 99.22° [**2a**: $(Cl–Ge–Cl)_{av.}$ = 101.37°]. Consequently, the Mo–Ge–Cl bond angles of ***trans*-4a** are more obtuse than those of **2a** having an average value of 118.41° [**2a**: $(Mo–Ge–Cl)_{av.}$ = 116.69°]. All these data suggest that hyperconjugation between the metal carbonyl fragment and the trichlorogermyl ligand becomes stronger, when the electron density at the metal center is enhanced.

Table 6
Selected bond lengths (pm) and bond angles (°) with estimated standard deviations for ***trans*-4a**

Mo(1)–C(1)	236.0(6)	C(6)–Mo(1)–P(1)	78.4(2)
Mo(1)–C(2)	232.9(5)	C(6)–Mo(1)–C(7)	110.8(2)
Mo(1)–C(3)	231.0(5)	C(6)–Mo(1)–Ge(1)	74.09(14)
Mo(1)–C(4)	229.6(5)	P(1)–Mo(1)–C(7)	77.5(2)
Mo(1)–C(5)	231.6(5)	P(1)–Mo(1)–Ge(1)	131.88(4)
Mo(1)–C(6)	196.4(6)	C(7)–Mo(1)–Ge(1)	76.5(2)
Mo(1)–C(7)	197.8(6)	Mo(1)–Ge(1)–Cl(1)	116.46(5)
Mo(1)–P(1)	247.43(13)	Mo(1)–Ge(1)–Cl(2)	121.30(6)
Mo(1)–Ge(1)	251.01(6)	Mo(1)–Ge(1)–Cl(3)	117.72(5)
Ge(1)–Cl(1)	220.2(2)	Cl(1)–Ge(1)–Cl(2)	98.85(8)
Ge(1)–Cl(2)	218.7(2)	Cl(1)–Ge(1)–Cl(3)	98.64(7)
Ge(1)–Cl(3)	219.7(2)	Cl(2)–Ge(1)–Cl(3)	99.76(9)

Reaction of **1b** and **1c** with EtNC in the presence of Me_3NO, which acts as a decarbonylating agent, gives the substitution products *cis*-CpW(CO)$_2$(EtNC)Cl (**5b**) and *cis*-Cp*W(CO)$_2$(EtNC)Cl (**5c**), respectively (Scheme 2).

These were purified by column chromatography on silica and isolated as orange-red, microcrystalline solids in 75% and 71% yields, respectively. Complexes **5b** and **5c** are thermally stable solids, which melt at 87°C and 137°C, respectively. They are soluble in CH_2Cl_2, THF and Et_2O, but sparingly soluble in pentane. The analogous molybdenum and tungsten iodo complexes to **5b** and **5c** have been previously prepared using the same procedure and have been shown to be useful starting materials for the synthesis of aminocarbyne-, η^2-imin-

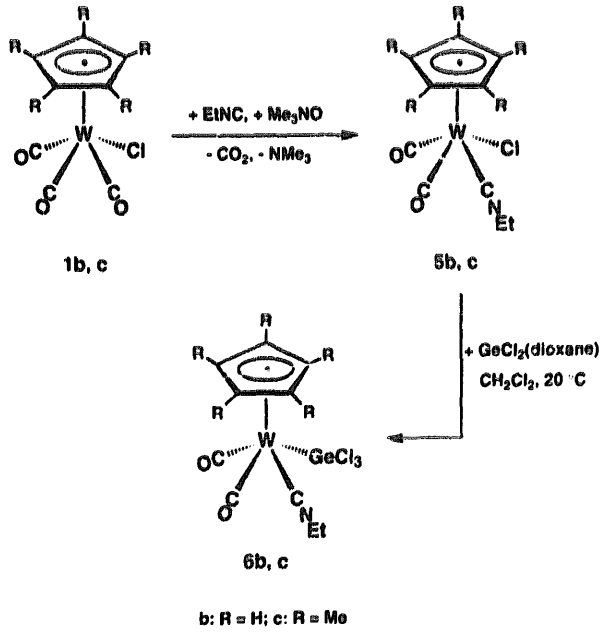

Scheme 2.

oacyl-, η^3-1-azaallyl-, η^2-diazabutadien-2-yl-, β-diiminato- and iminocarbene complexes [35,36].

Treatment of **5b** and **5c** with one equivalent $GeCl_2$(dioxane) in CH_2Cl_2 at room temperature afforded selectively the trichlorogermyl complexes *cis*-$CpW(CO)_2(EtNC)GeCl_3$ (**6b**) and *cis*-$Cp^*W(CO)_2(EtNC)GeCl_3$ (**6c**), respectively (Scheme 2). Again IR monitoring of these reactions revealed the clean conversion of the starting materials to the products, which were isolated as yellow, microcrystalline solids in 90% and 95% yields, respectively. Both compounds are thermally stable solids, which are soluble in CH_2Cl_2, sparingly soluble in Et_2O, but insoluble in pentane and melt at 97°C and 120°C, respectively. IR spectra of the cooled melts in CH_2Cl_2 gave no evidence for an isomerization to the corresponding *trans*-isomers. However, compound **6b** isomerizes in the molten state at higher temperature (122°C) to the *trans*-isomer as shown by a coupled TG/DTA investigation, the results of which will be published elsewhere.

Complexes **6b** and **6c** are distinguished by two ν(CO) absorption bands in the IR spectra, the higher energy absorption of the symmetric ν(CO) vibration being more intense than the lower energy absorption of the antisymmetric ν(CO) vibration as expected for a *cis*-isomer. The ν(CO) absorption bands of **6b** and **6c** appear at higher wavenumbers than those of the chloro complexes **5b** and **5c** indicating that insertion of $GeCl_2$ into the M–Cl bond causes a decrease of the electron density at the metal center (Table 1). The same trend was observed for the PMe_3 containing complexes **3a** and ***cis*-4a**. In addition, the ^{13}C-NMR spectra of **6b** and **6c** display two carbonyl-carbon resonances at δ 222.5 and 224.5 and 225.8 and 229.5, respectively, confirming along with the IR spectra the *cis* arrangement of the carbonyl ligands. These resonances appear at higher field than those of the chloro complexes **5b** and **5c** because of the weaker metal–carbonyl back bonding in **6b** and **6c** (Table 3) [16,31]. For the same reason, the metal-bound isonitrile–carbon nucleus of **6b** and **6c** (δ 142.5 and 148.9, respectively) is more shielded than that of **5b** and **5c** (δ 150.6 and 155.9, respectively) [37].

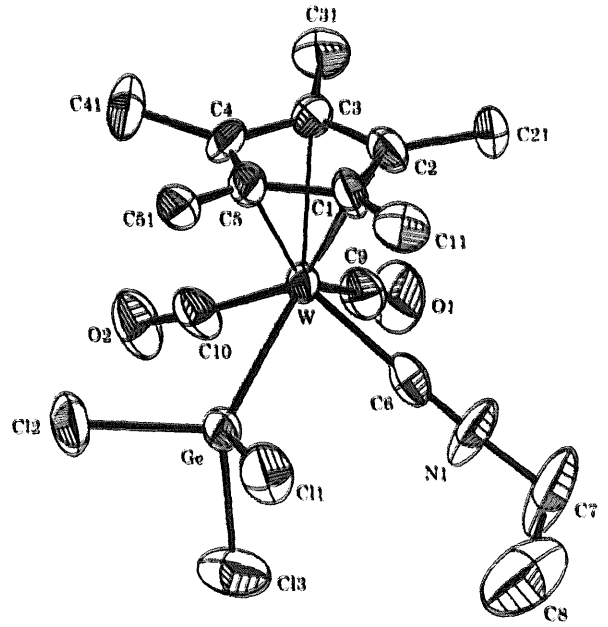

Fig. 4. ZORTEP plot of the structure of **6c** with thermal ellipsoids drawn at the 50% probability level.

Table 7
Selected bond lengths (pm) and bond angles (°) with estimated standard deviations for **6c**

W–C(1)	231(2)	C(6)–W–C(9)	78.7(8)
W–C(2)	230(2)	C(6)–W–C(10)	122.6(8)
W–C(3)	230(2)	C(6)–W–Ge	75.2(4)
W–C(4)	230(2)	C(9)–W–C(10)	75.8(8)
W–C(5)	236(2)	C(9)–W–Ge	120.7(6)
W–C(6)	205(2)	C(10)–W–Ge	75.5(5)
W–C(9)	195(2)	W–Ge–Cl(1)	118.0(2)
W–C(10)	197(2)	W–Ge–Cl(2)	119.0(2)
W–Ge	254.4(2)	W–Ge–Cl(3)	118.6(2)
Ge–Cl(1)	220.8(6)	Cl(1)–Ge–Cl(2)	98.6(2)
Ge–Cl(2)	219.6(5)	Cl(1)–Ge–Cl(3)	99.1(3)
Ge–Cl(3)	218.5(6)	Cl(2)–Ge–Cl(3)	99.7(3)

The solid-state structure of **6c** was determined by a single-crystal X-ray diffraction study. Suitable single crystals were obtained after slow evaporation of a CH_2Cl_2 solution of **6c** at room temperature. A ZORTEP drawing of **6c** with the atom-labeling scheme adopted is shown in Fig. 4. Selected bond lengths and angles of **6c** are listed in Table 7.

Complex **6c** shows the expected square-pyramidal coordination geometry of a 'four-legged piano-stool' complex with a *cis* arrangement of the trichlorogermyl and the ethyl isonitrile ligand. A comparison of the structural parameters of the trichlorogermyl ligand in **2c** and in **6c** shows that substitution of a carbonyl group from the *cis*-position relative to the trichlorogermyl ligand by an ethyl isonitrile ligand results in a shortening of the W–Ge bond [**2c**: $(W–Ge)_{av.}$ = 256.2 pm; **6c**: W–Ge = 254.4(2) pm], an elongation of the Ge–Cl bonds [**2c**: $(Ge–Cl)_{av.}$ = 217.9 pm; **6c**: $(Ge–Cl)_{av.}$ = 219.6 pm] and a slightly larger distortion of the tetrahedral environment of the germanium atom. Thus, the Cl–Ge–Cl bond angles of **6c** are slightly more acute than those of **2c** having an average value of 99.1° [**2c**: $(Cl–Ge–Cl)_{av.}$ = 100.2°]. Consequently, the W–Ge–Cl bond angles of **6c** are slightly more obtuse than those of **2c** having an average value of 118.5° [**2c**: $(W–Ge–Cl)_{av.}$ = 117.6°]. These structural effects could be explained by a stronger hyperconjugation between the metal carbonyl fragment and the trichlorogermyl ligand in **6c** (see also comparison of the structures of **2a** and ***trans*-4a** above).

In order to find out whether the presented $GeCl_2$ insertion reaction of Group VI transition metal chloro

complexes is a more convenient method for the synthesis of trichlorogermyl complexes than the salt elimination reaction of $GeCl_4$ with an appropriate Group VI transition metal complex anion, the carbonyl metallate $Na[Cp^* W(CO)_2(EtNC)]$ (**7c**) was prepared by reduction of the chloro complex **5c** in THF with an excess of sodium and was treated at −40°C with one equivalent of $GeCl_4$. IR monitoring of this reaction revealed not only the formation of the desired trichlorogermyl complex **6c** but also of the chloro complex **5c** (Eq. (4); the filled circles on the cyclopentadiene ligand represent methyl groups).

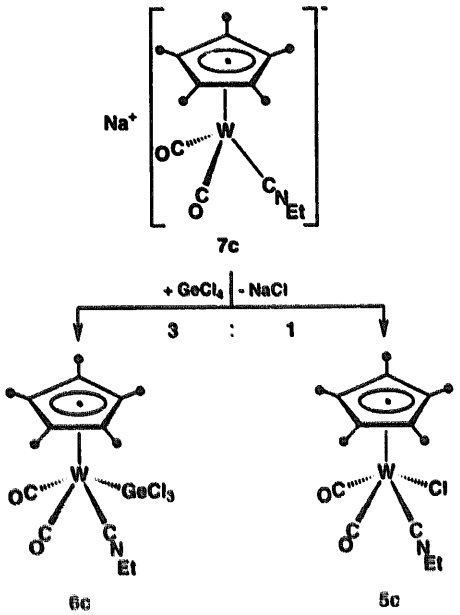

(4)

The complexes **5c** and **6c** were easily separated taking advantage of the much higher solubility of the chloro complex **5c** in an Et_2O/pentane (1/1) mixture and were isolated in 24% and 69% yields, respectively. The formation of **5c** indicates that $GeCl_4$ can act also as an oxidizing agent towards a group VI transition metal complex anion limiting the use of the salt elimination reaction for the preparation of trichlorogermyl complexes. In these cases, the '$GeCl_2$ insertion' route is by far a more convenient method, since $GeCl_2$ (dioxane) can be easily prepared from $GeCl_4$ [38] and reacts rapidly and selectively with the chloro complex employed. In fact, recent studies show that the '$GeCl_2$ insertion' method can be extended to more 'electron-rich' molybdenum and tungsten chloro complexes of the type $(\eta^5\text{-}C_5R_5)M(CO)L_2Cl$ (R = H, Me; L = EtNC, PMe_3) giving access to trichlorogermyl complexes, which are attractive starting materials for the synthesis of germylene and germylyne complexes.

3. Experimental

Standard inert-atmosphere techniques were used for all syntheses and sample manipulations. The solvents were dried by standard methods (pentane over CaH_2, Et_2O DME, and THF over Na/benzophenone, CH_2Cl_2 over P_2O_5 and Na/Pb alloy), distilled under argon and stored over 4 Å molecular sieves prior to use. All column chromatography was carried out in a thermostatted column of 20 cm length and 2.0 cm diameter. The stationary phase was silica (Merck, 0.063–0.2 mm) which was degassed, dried in vacuo at room temperature and saturated with argon.

Elemental analyses were obtained from the Zentrale Analytische Gruppe des Instituts für Chemie der Humboldt Universität zu Berlin. IR spectra were recorded on a Bruker IFS-55 spectrometer. ^{1}H-, $^{13}C\{^1H\}$- and $^{31}P\{^1H\}$-NMR spectra were recorded on a Bruker AM-300 spectrometer in dry deoxygenated methylene-d_2-chloride, benzene-d_6 and chloroform-d_1. The ^{1}H- and $^{13}C\{^1H\}$-NMR spectra were calibrated against the solvent signals (methylene-d_2-chloride, δ_H 5.32 and δ_C 53.8 ppm; benzene-d_6, δ_H 7.15 and δ_C 128.0 ppm; chloroform-d_1 δ_H 7.24 and δ_C 77.0 ppm) and the $^{31}P\{^1H\}$-NMR spectra against an external 85% H_3PO_4 aqueous solution. Mass spectra were obtained with a HP 5995A spectrometer; m/z values are given relative to the ^{98}Mo, ^{184}W, ^{74}Ge and ^{35}Cl isotopes. Melting points were determined using a Büchi 530 melting point apparatus and are not corrected. The samples were sealed in capillary tubes under argon.

The complexes **1a** and **1c** were obtained from $Mo(CO)_6$ and $W(CO)_6$ in 80% and 85% overall yields respectively, following the procedure described below for $CpW(CO)_3Cl$ (**1b**). $GeCl_2$(dioxane) was prepared following the procedure of Nefedov et al. [38]. $PhICl_2$, PMe_3 and EtNC were prepared according to published procedures [39–41]. $Me_3NO \cdot 2H_2O$ was purchased from Sigma–Aldrich Chemie and dehydrated by sublimation in vacuo before use. $GeCl_4$ was used as supplied from Heraeus Feinchemikalien und Forschungsbedarf.

3.1. $CpW(CO)_3Cl$ (1b)

A suspension of 1.02 g (11.58 mmol) of NaCp and 3.39 g (9.63 mmol) of $W(CO)_6$ in 100 ml of DME was refluxed for 15 h. During this time evolution of gas (CO) was observed and the colour of the solution changed to yellow-brown. After all $W(CO)_6$ had been consumed (disappearance of the ν(CO) absorption of $W(CO)_6$ in the IR spectrum of the reaction solution at 1976 cm^{-1}), the solution was cooled to −78°C and 2.91 g (10.60 mmol) of freshly prepared $PhICl_2$ were added in small portions to the solution. The resulting

suspension was allowed to warm to ambient temperature and stirred for 30 min. Completion of the reaction was confirmed by IR spectroscopy (replacement of the ν(CO) absorptions of $Na[CpW(CO)_3]$ at 1893, 1791, 1779 and 1725 cm^{-1} by those of the product **1b** at 2044 and 1953 cm^{-1}). The resulting red suspension was treated at −30°C with ca. 30 g of silica gel and the solvent then removed in vacuo at room temperature. The obtained powder was poured into a chromatographic column, which was filled with a suspension of silica gel in Et_2O, and the product was eluted with Et_2O. The red eluate was evaporated to dryness and the residue was washed twice with small portions of cold (−78°C) pentane to afford complex **1b** as a red, microcrystalline solid. Yield: 3.15 g (89% rel. to $W(CO)_6$). The product was characterized by IR spectroscopy and was used for all experiments described below.

3.2. $CpMo(CO)_3GeCl_3$ (2a)

A mixture of 198 mg (0.71 mmol) of **1a** and 164 mg (0.71 mmol) of $GeCl_2$(dioxane) was suspended at −78°C in 30 ml of CH_2Cl_2 and the suspension was allowed to warm to room temperature and stirred for 2 h. During this time the dark-red solution brightened. Completion of the reaction was confirmed by IR spectroscopy. The solution was then filtered from some insoluble brown material through a filter canula and the filtrate was evaporated to dryness. The residue was washed twice with 5 ml of an Et_2O/pentane (1/3) mixture to afford complex **2a** as a yellow, microcrystalline solid. M.p.: 129°C. Yield: 290 mg (97%). Found: C, 22.40; H, 1.21; Cl, 25.04; $C_8H_5Cl_3GeMoO_3$ (424.03). Calcd. : C, 22.66; H, 1.19; Cl, 25.08%. EI-MS (70 eV): m/z 426 $[M^+]$, 398 $([M-CO]^+)$, 391 $([M-Cl]^+)$, 370 $([M-2\ CO]^+)$, 342 $([M-3\ CO]^+)$, 307 $([M-3\ CO-Cl]^+)$, 254 $([M-CO-GeCl_2]^+)$, 226 $([M-2\ CO-GeCl_2]^+)$, 198 $([M-3\ CO-GeCl_2]^+)$ (base peak).

3.3. $CpW(CO)_3GeCl_3$ (2b)

Following the procedure described above for the synthesis of **2a**, complex **2b** was obtained as a yellow, microcrystalline solid after treatment of 906 mg (2.46 mmol) of **1b** with 569 mg (2.46 mmol) of $GeCl_2$(dioxane) in 50 ml of CH_2Cl_2 at room temperature for 2 h. Yield: 1.21 g (96%). M.p.: 154°C. Found: C, 18.47; H, 1.17; Cl, 20.60; $C_8H_5Cl_3GeO_3W$ (511.94). Calcd. : C, 18.77; H, 0.98; Cl, 20.78%. EI-MS (70 eV): m/z 512 $[M^+]$, 477 $([M-Cl]^+)$, 428 $([M-3\ CO]^+)$, 368 $([M-GeCl_2]^+)$, 340 $([M-GeCl_2-CO]^+)$, 393 $([M-Cl-3\ CO]^+)$, 312 $([M-GeCl_2-2\ CO]^+)$, 284 $([M-GeCl_2-3\ CO]^+)$ (base peak).

3.4. $Cp^*W(CO)_3GeCl_3$ (2c)

Following the procedure described above for the synthesis of **2a**, complex **2c** was obtained as a yellow, microcrystalline solid after treatment of 288 mg (0.66 mmol) of **1c** with 153 mg (0.66 mmol) of $GeCl_2$(dioxane) in 40 ml of CH_2Cl_2 at room temperature for **2d**. Yield: 306 mg (80%). M.p.: 160°C. Found: C, 25.67; H, 2.68; $C_{13}H_{15}Cl_3GeO_3W$ (582.08). Calcd. : C, 26.82; H, 2.60%. EI-MS (70 eV): m/z 582 $[M^+]$, 547 $([M-Cl]^+)$, 519 $([M-Cl-CO]^+)$, 491 $([M-Cl-2\ CO]^+)$, 463 $([M-Cl-3CO]^+)$, 438 $([M-GeCl_2]^+)$, 410 $([M-GeCl_2-CO]^+)$, 403 $([M-GeCl_3]^+)$ 382 $([M-GeCl_2-2\ CO]^+)$, 354 $([M-GeCl_2-3\ CO]^+)$ (base peak).

3.5. cis-$CpMo(CO)_2(PMe_3)Cl$ (3a) and trans-$[CpMo(CO)_2(PMe_3)_2]Cl$ (3a′)

A solution of 380 mg (1.35 mmol) of **1a** in 30 ml of THF was treated at room temperature with 0.18 ml (1.74 mmol) of PMe_3 and the red solution stirred for 2 h. During this time evolution of gas (CO) and precipitation of a yellow solid was observed. Completion of the reaction was confirmed by IR spectroscopy. The suspension was then evaporated to dryness and the residue treated with 30 ml of Et_2O. The solution was filtered through a filter canula leaving an insoluble solid, which was washed once with Et_2O and dried in vacuo to afford complex **3a′** as a yellow solid. M.p.: 203°C (dec.). Yield: 190 mg (35%). Found: C, 38.41; H, 5.82; Cl, 7.87; $C_{13}H_{24}ClMoO_2P_2$ (404.66). Calcd. : C, 38.59; H, 5.73; Cl, 8.76%.

The Et_2O filtrate was filtered over a short layer of silica (2 × 2 cm) and the orange-red filtrate evaporated to dryness to give complex **3a** as an orange-red, microcrystalline solid. M.p.: 156°C (dec.). Yield: 200 mg (45%). Found: C, 36.41; H, 4.07; Cl, 11.67; $C_{10}H_{14}ClMoO_2P$ (328.59). Calcd. : C, 36.55; H, 4.29; Cl, 10.79%. EI-MS (70 eV): EI-MS (70 eV): m/z 330 $[M^+]$, 302 $([M-CO]^+)$, 274 $([M-2\ CO]^+)$, 198 $([M-2\ CO-PMe_3]^+)$ (base peak).

3.6. cis-$CpMo(CO)_2(PMe_3)GeCl_3$ (cis-4a)

A mixture of 116 mg (0.35 mmol) of **3a** and 82 mg (0.35 mmol) of $GeCl_2$(dioxane) was suspended at −78°C in 20 ml of CH_2Cl_2 and the suspension was allowed to warm to room temperature and stirred for 1 h. During this time the colour of the solution changed from red to yellow-orange. Completion of the reaction was confirmed by IR spectroscopy. The solution was then filtered through a filter canula and the filtrate was evaporated to dryness. The residue was washed once with a Et_2O/pentane mixture (1:1) to afford complex

***cis*-4a** as a yellow, microcrystalline solid. M.p.: 226°C (isomerization). Yield: 150 mg (91%). Found: C, 24.62; H, 2.78; $C_{10}H_{14}Cl_3GeMoPO_2$ (472.10). Calcd. : C, 25.44; H, 2.99%. EI–MS (70 eV): m/z 474 $[M^+]$, 439 $([M-Cl]^+)$, 304 $([M-CO-GeCl_2]^+)$, 276 $([M-2\ CO-GeCl_2]^+)$, 200 $([M-2\ CO-GeCl_2-PMe_3]^+)$ (base peak).

3.7. *trans-CpMo(CO)$_2$(PMe$_3$)GeCl$_3$ (trans-4a)*

A solution of 50 mg (0.11 mmol) of ***cis*-4a** in 5 ml CH_2Cl_2 was stirred at room temperature. After 2 days the isomerization to the *trans*-isomer was complete as confirmed by IR spectroscopy. The solvent was evaporated to dryness and the residue washed with pentane to give quantitatively ***trans*-4a** as a yellow, microcrystalline solid. M.p.: 232°C. The complex was characterized by IR, ^{1}H-, ^{13}C- and ^{31}P-NMR spectroscopy.

3.8. *cis-CpW(CO)$_2$(EtNC)Cl (5b)*

A solution of 1.08 g (2.93 mmol) of **1b** in 50 ml of CH_2Cl_2 was treated at −78°C with 0.28 ml (3.77 mmol) of EtNC and 308 mg (4.10 mmol) of Me_3NO and then allowed to warm to room temperature and stirred for 3 h until reaction was complete (IR monitoring). To the red solution were added at −30°C ca. 20 g of silica and the solvent was stripped off in vacuo at room temperature. The resulting powder was poured into a chromatographic column, which was filled with a suspension of silica gel in Et_2O, and the product was eluted with Et_2O. The red eluate was concentrated in vacuo, cooled to −78°C, and cold pentane was slowly added to complete precipitation of **5b**. Orange-red, microcrystalline solid. M.p.: 87°C. Yield: 870 mg (75%). Found: C, 30.92; H, 2.71; N, 3.61; $C_{10}H_{10}ClNO_2W$ (395.50). calcd.: C, 30.37; H, 2.55; N, 3.54%.

3.9. *cis-Cp*W(CO)$_2$(EtNC)Cl (5c)*

Following the procedure described above for the synthesis of **5b** complex **5c** was obtained as an orange-red, microcrystalline solid, after treatment of 1.69 g (3.85 mmol) of **1c** with 0.32 ml (4.25 mmol) of EtNC and 377 mg (5.02 mmol) of Me_3NO in CH_2Cl_2 for 3h. M.p.: 137°C. Yield: 1.28 g (71%). $C_{15}H_{20}ClNO_2W$ (465.63). EI–MS (70 eV): m/z 465 $[M^+]$, 437 $([M-CO]^+)$, 409 $([M-2\ CO]^+)$.

3.10. *cis-CpW(CO)$_2$(EtNC)GeCl$_3$ (6b)*

A mixture of 325 mg (0.82 mmol) of **5b** and 210 mg (0.91 mmol) of $GeCl_2$(dioxane) was suspended at −78°C in 20 ml of CH_2Cl_2 and the suspension was allowed to warm to room temperature and stirred for 2 h. During this time the colour of the solution changed from dark-red to orange. Completion of the reaction was confirmed by IR spectroscopy. The solution was then filtered through a filter canula and the filtrate was evaporated to dryness. The residue was washed twice with 10 ml of pentane to afford complex **6b** as a pale-yellow, microcrystalline solid. M.p.: 97°C. Yield: 400 mg (90%). Found: C, 21.01; H, 1.85; Cl, 20.75; N, 2.75; $C_{10}H_{10}Cl_3GeNO_2W$ (539.01). Calcd. : C, 22.28; H, 1.87; Cl, 19.73; N, 2.60%. EI–MS (70 eV): m/z 539 $[M^+]$, 504 $([M-Cl]^+)$, 413 $([M-2\ Cl-2\ CO]^+)$, 395 $([M-GeCl_2]^+)$, 385 $([M-2\ Cl-2\ CO-C_2H_4]^+)$, 367 $([M-GeCl_2-CO]^+)$, 358 $([M-2\ Cl-2\ CO-EtNC]^+)$, 339 $([M-GeCl_2-2\ CO]^+)$ (base peak), 284 $([M-GeCl_2-2\ CO-EtNC]^+)$, 249 $([M-GeCl_2-2\ CO-EtNC-Cl]^+)$.

3.11. *cis-Cp*W(CO)$_2$(EtNC)GeCl$_3$ (6c) from Na[Cp*W(CO)$_2$(EtNC)] (7c) and GeCl$_4$*

A solution of 313 mg (0.67 mmol) of **5c** in 30 ml of THF was treated with 65 mg (2.83 mmol) of sodium powder and stirred for 24 h at room temperature. During this time the colour of the solution changed from red to yellow-brown and precipitation of NaCl was observed. Completion of the reaction and selective formation of the metallate **7c** was confirmed by IR spectroscopy. The precipitate was allowed to settle and the solution was filtered through a filter canula. The filtrate was slowly added at −40°C to a solution of 0.08 ml (0.70 mmol) of $GeCl_4$ in 15 ml of THF and the mixture was warmed to room temperature and stirred for 1.5 h. Completion of the reaction to give **5c** and **6c** was revealed by IR spectroscopy. The suspension was then evaporated to dryness and the residue dissolved in CH_2Cl_2. The cloudy solution was filtered from NaCl and the filtrate evaporated to dryness. The residue was washed three times with a Et_2O/pentane mixture (1:1) to remove complex **5c** and dried in vacuo to afford complex **6c** as a yellow, microcrystalline solid. M.p.: 120°C. Yield: 281 mg (69%). Found: C, 29.22; H, 3.48; Cl, 16.94; N, 2.25; $C_{15}H_{20}Cl_3GeNO_2W$ (609.15). calcd.: C, 29.58; H, 3.31; Cl, 17.46; N 2.30%. EI–MS (70 eV): m/z 609 $[M^+]$, 574 $([M-Cl]^+)$, 465 $([M-GeCl_2]^+)$, 437 $([M-GeCl_2-CO]^+)$, 409 $([M-GeCl_2-2\ CO]^+)$, 381 $([M-GeCl_2-2\ CO-C_2H_4]^+)$ (base peak), 354 $([M-GeCl_2-2\ CO-EtNC]^+)$.

The combined Et_2O/pentane (1:1) washings were evaporated to dryness to give 75 mg of the chloro complex **5c** (yield: 24%).

3.12. *cis-Cp*W(CO)$_2$(EtNC)GeCl$_4$ (6c) from 5c and GeCl$_2$(dioxane)*

A mixture of 203 mg (0.50 mmol) of **5c** and 116 mg (0.50 mmol) of $GeCl_2$(dioxane) was suspended at −78°C in 40 ml of CH_2Cl_2 and the suspension was

Table 8
Summary of crystallographic data for the complexes **2a**, **2c**, ***trans*-4a** and **6c**

	2a	**2c**	***trans*-4a**	**6c**
Empirical formula	$C_8H_5Cl_3GeMoO_3$	$C_{13}H_{15}Cl_3GeO_3W$	$C_{10}H_{14}Cl_3GeMoO_2P$	$C_{15}H_{20}Cl_3GeNO_2W$
Molecular weight	424.02	582.04	472.08	609.13
Crystal colour	yellow	yellow	yellow	yellow
Crystal size (mm)	0.38 × 0.29 × 0.19	0.65 × 0.47 × 0.30	1.14 × 0.76 × 0.38	0.34 × 0.25 × 0.15 mm
Crystal system	monoclinic	orthorhombic	monoclinic	monoclinic
Space group	$P2_1/n$ (no. 14)	$Pca2_1$ (no. 29)	$P2_1/c$ (no. 14)	$P2_1$ (no. 4)
a (Å)	9.2796(12)	17.147(4)	12.5742(11)	8.0350(11)
b (Å)	15.557(2)	12.309(3)	14.7964(5)	16.779(3)
c (Å)	9.3186(13)	17.253(11)	18.5255(4)	8.4281(13)
β (°)	94.151(12)		92.005(4)	113.838(11)
V (Å^3)	1341.8(3)	3641(3)	3444.6(3)	1039.3(3)
Z	4	8	8	2
$\rho_{calcd.}$ (g/cm^3)	2.099	2.123	1.821	1.946
$\mu_{MoK\alpha}$ (mm^{-1})	3.599	8.408	2.898	7.094
$F(000)$	808	2192	1840	580
2Θ min./max. (°)	5.50	3.54	3.50	5.48
hkl range	−11, 11/0, 18/0, 11	0, 21/0, 15/−21, 0	−14, 14/0, 17/−18, 21	−9, 8/0, 19/0, 9
Total data	2500	4627	7185	1963
Data unique ($I > 2\sigma I$)	2354	4107 [R(int) = 0.0128]	6042 [R(int) = 0.1821]	1692 [R(int) = 0.1564]
Min./max. density (eÅ^{-3})	1.384/−0.803	1.017/−0.671	0.981/−1.987	1.172/−1.508
No. of parameters refined	146	380	326	208
Absorption corr.	ψ-scan	DIFABS	ψ-scan	ψ-scan
Min./max.	0.617/0.993	0.760/1.344	0.3328/10.9437	0.4983/10.9959
Extinction coeff. [a]	0.0045(8)	0.00017(6)	0.0035(3)	
R_1 [b] [$I > 2\sigma(I)$]	0.0525	0.0334	0.0532	0.0381
wR_2 [c]	0.1254	0.0915	0.1411	0.0905
GOF [d]	1.100	0.771	1.083	1.086

[a] $F_c^* = kF_c[1 + 0.001 \times F_c^2\lambda^3/\sin(2\Theta)]^{-1/4}$.
[b] $R_1 = \Sigma||F_o| - |F_c||/\Sigma|F_o|$.
[c] $wR_2 = [\Sigma[w(F_o^2 - F_c^2)^2]/\Sigma[w(F_o^2)^2]]^{1/2}$.
[d] $GOF = S = [\Sigma[w(F_o^2 - F_c^2)^2]/(n - p)]^{1/2}$.

allowed to warm to room temperature and stirred for 24 h. During this time the colour of the solution changed from dark-red to orange. Completion of the reaction was confirmed by IR spectroscopy. The solution was then filtered through a filter canula and the filtrate was evaporated to dryness. The residue was washed twice with a Et_2O/pentane mixture (1:1) to afford complex **6c** as a yellow, microcrystalline solid. Yield: 290 mg (95%). The product was characterized by IR and NMR spectroscopy.

4. Crystal structure determinations of 2a, 2c, *trans*-4a and 6c

A summary of the crystal data, data collection and refinement for all structures is given in Table 8.

Data collection was performed on a STOE STADI4 four circle diffractometer at ambient temperature and with graphite monochromated MoK_α radiation (λ = 0.71073 Å). Lattice parameters were determined from the setting angles of 21–30 reflections in the range of $24° \leq 2\Theta \leq 36°$. Data were collected in the $\bar{\omega}$-2Θ scan mode. After every 2 to 3 hours three standard reflections were monitored and the crystal reoriented in case of deviation between 0.1° and 0.15°. Intensity data were corrected for Lorentz and polarization effects and ab-

Table 9
Atomic coordinates (×10^4) and equivalent isotropic displacement parameters (pm^2 × 10^7) for **2a**

Atom	x	y	z	U_{eq} [a]
Mo	2129(1)	1197(1)	2664(1)	35(1)
Ge	1189(1)	2301(1)	4384(1)	46(1)
Cl(1)	−687(3)	3072(2)	3681(3)	70(1)
Cl(2)	595(3)	1792(2)	6431(3)	78(1)
Cl(3)	2701(3)	3315(2)	5082(3)	87(1)
C(1)	4401(12)	675(10)	2395(13)	87(4)
C(2)	4560(11)	1269(8)	3452(16)	86(4)
C(3)	3823(13)	993(8)	4595(11)	83(4)
C(4)	3217(11)	191(7)	4248(13)	77(3)
C(5)	3607(13)	3(7)	2841(13)	86(4)
C(6)	136(10)	811(5)	2984(9)	53(2)
O(1)	−989(8)	567(5)	3207(8)	82(2)
C(7)	1461(11)	833(6)	656(10)	59(2)
O(2)	1094(9)	646(5)	−486(7)	87(2)
C(8)	2022(9)	2310(5)	1598(9)	52(2)
O(3)	1957(8)	2943(4)	951(8)	73(2)

[a] U_{eq} is defined as one-third of the trace of the orthogonalized U_{ij} tensor.

sorption. The input files for the SHELX programs were prepared with the program UTILITY [42]. Structure solution was performed with the Patterson method (SHELXS-86) [43] and subsequent difference-fourier synthesis (SHELXL-93) [44]. Refinement on F^2 was carried out by full-matrix least squares techniques (SHELXL-93). Non-hydrogen atoms were refined with anisotropic thermal parameters. Hydrogen atoms were included using a riding model with d(C–H) = 0.96 Å and U_{iso} = 0.08 Å^2. Neutral atom scattering factors were taken from Cromer and Mann [45]. Geometrical calculations and illustrations were performed with PLATON [46] and ZORTEP [47].

Table 10
Atomic coordinates ($\times 10^4$) and equivalent isotropic displacement parameters (pm$^2 \times 10^7$) for **2c**

Atom	x	y	z	U_{eq} [a]
W(1)	8782(1)	9389(1)	10004(1)	37(1)
Ge(1)	9637(1)	9765(1)	11193(1)	42(1)
Cl(1)	10348(3)	8409(3)	11609(2)	66(1)
Cl(2)	10527(2)	11026(4)	11113(3)	67(1)
Cl(3)	9062(3)	10257(4)	12264(3)	71(1)
C(1)	8499(8)	11273(11)	9921(11)	51(3)
C(11)	8749(11)	12205(13)	10416(11)	69(5)
C(2)	8856(8)	10928(11)	9203(8)	45(3)
C(21)	9579(10)	11425(14)	8863(10)	66(4)
C(3)	8342(10)	10152(11)	8866(9)	50(3)
C(31)	8471(14)	9646(15)	8076(8)	73(5)
C(4)	7689(8)	9988(12)	9371(10)	54(3)
C(41)	6985(10)	9293(18)	9180(11)	73(5)
C(5)	7798(8)	10661(11)	10038(11)	47(3)
C(51)	7213(11)	10920(14)	10641(12)	67(5)
C(10)	8258(10)	8597(15)	10894(10)	65(4)
O(1)	7951(9)	8167(13)	11366(9)	97(5)
C(20)	9866(10)	8962(10)	9708(8)	53(4)
O(2)	10502(7)	8825(10)	9484(7)	70(3)
C(30)	8637(9)	7902(14)	9565(11)	62(4)
O(3)	8528(10)	7077(12)	9292(9)	96(4)
W(2)	11731(1)	4875(1)	7968(1)	37(1)
Ge(2)	10898(1)	4787(1)	9198(1)	49(1)
Cl(4)	10870(4)	6201(4)	9954(4)	98(2)
Cl(5)	11172(4)	3520(4)	10034(3)	88(1)
Cl(6)	9656(3)	4512(4)	9051(4)	93(2)
C(6)	10982(7)	6401(11)	7571(8)	44(3)
C(61)	10304(9)	6969(12)	7963(12)	66(4)
C(7)	11768(8)	6700(12)	7571(12)	63(5)
C(71)	12095(11)	7620(14)	8051(18)	115(10)
C(8)	12141(11)	6000(20)	6988(15)	96(8)
C(81)	12978(15)	6109(30)	6762(25)	220(29)
C(9)	11581(13)	5271(17)	6693(12)	73(5)
C(91)	11690(25)	4606(30)	5955(15)	183(23)
C(10)	10857(10)	5546(12)	7039(10)	57(4)
C(101)	10088(16)	5051(21)	6819(16)	100(8)
O(4)	11016(7)	2541(8)	7952(10)	81(4)
C(40)	11267(8)	3399(12)	7976(9)	54(3)
C(50)	12432(10)	5202(13)	8833(13)	66(5)
O(5)	12842(9)	5470(17)	9324(10)	106(6)
C(60)	12645(8)	3932(13)	7725(9)	55(4)
O(6)	13159(7)	3403(12)	7548(10)	92(5)

[a] U_{eq} is defined as one-third of the trace of the orthogonalized U_{ij} tensor.

Table 11
Atomic coordinates ($\times 10^4$) and equivalent isotropic displacement parameters (pm$^2 \times 10^7$) for ***trans*-4a**

Atom	x	y	z	U_{eq} [a]
Mo(1)	2922(1)	7545(1)	2323(1)	36(1)
Ge(1)	3044(1)	8000(1)	1024(1)	44(1)
Cl(1)	4040(1)	9186(1)	804(1)	67(1)
Cl(2)	1627(2)	8375(2)	374(1)	100(1)
Cl(3)	3770(2)	7037(1)	284(1)	75(1)
C(1)	1522(6)	8289(5)	2897(4)	75(2)
C(2)	2255(7)	8010(4)	3420(3)	72(2)
C(3)	3206(6)	8451(4)	3328(3)	67(2)
C(4)	3081(6)	9011(4)	2717(3)	67(2)
C(5)	2049(6)	8910(4)	2454(3)	69(2)
C(6)	4422(5)	7393(4)	2088(3)	54(1)
O(1)	5302(4)	7376(4)	1964(3)	92(2)
C(7)	2018(5)	6646(4)	1803(3)	55(1)
O(2)	1451(4)	6145(4)	1528(3)	92(2)
P(1)	3383(1)	6124(1)	2965(1)	52(1)
C(8)	4284(6)	6265(5)	3736(3)	81(2)
C(9)	4028(6)	5281(4)	2431(4)	83(2)
C(10)	2304(6)	5509(5)	3341(4)	86(2)
Mo(2)	2070(1)	2552(1)	169(1)	37(1)
Ge(2)	1744(1)	2114(1)	1446(1)	51(1)
Cl(4)	1524(2)	3205(2)	2224(1)	95(1)
Cl(5)	2941(1)	1295(1)	2041(1)	79(1)
Cl(6)	354(2)	1284(2)	1661(1)	108(1)
C(11)	3123(7)	1534(7)	−444(6)	105(3)
C(12)	2457(11)	1047(5)	12(4)	112(4)
C(13)	1426(8)	1185(5)	−234(4)	85(2)
C(14)	1466(7)	1734(5)	−833(3)	77(2)
C(15)	2480(7)	1951(5)	−950(4)	76(2)
C(16)	725(5)	3175(4)	395(3)	53(1)
O(3)	−61(4)	3510(4)	495(3)	84(1)
C(17)	3235(5)	3145(4)	736(3)	52(1)
O(4)	3941(4)	3464(4)	1039(3)	82(1)
P(2)	2243(1)	4019(1)	−448(1)	51(1)
C(18)	1328(6)	4207(5)	−1203(3)	82(2)
C(19)	2033(7)	4990(4)	116(4)	89(2)
C(20)	3520(6)	4228(5)	−814(4)	85(2)

[a] U_{eq} is defined as one-third of the trace of the orthogonalized U_{ij} tensor.

In the final stages of the refinement data for **2a**, **2c** and ***trans*-4a** were corrected for secondary extinction effects. **2c** and ***trans*-4a** crystallize with two independent molecules in the asymmetric unit. Complexes **2c** and **6c** crystallize in the non-centrosymmetric space groups Pca2$_1$ and P2$_1$, respectively. The absolute structure parameter [48] of χ = 0.02(2) for **2c** and χ = 0.01(2) for **6c** confirmed the correct positions for the atoms in the structure. The anisotropic displacement parameters for the atoms C7 and C8 of the ethyl group in compound **6c** are rather enlarged. However, using a split atom model was not successful. The bond length C7–C8 was idealized with 151 pm.

Final positional and equivalent isotropic thermal parameters are given in Table 9 for **2a**, Table 10 for **2c**, Table 11 for ***trans*-4a** and in Table 12 for **6c**.

Crystallographic data (excluding structure factors) for the structures reported in this paper have been

Table 12
Atomic coordinates ($\times 10^4$) and equivalent isotropic displacement parameters ($pm^2 \times 10^7$) for **6c**

Atom	x	y	z	U_{eq} [a]
W	1705(1)	−6(1)	8646(1)	39(1)
Ge	437(2)	1253(1)	6891(2)	48(1)
Cl(1)	2352(8)	2229(3)	7083(7)	79(2)
Cl(2)	−903(8)	1168(4)	4052(6)	83(2)
Cl(3)	−1621(10)	1933(4)	7390(9)	98(2)
C(1)	4700(18)	−7(17)	8966(17)	52(3)
C(11)	6032(31)	648(13)	9541(31)	82(6)
C(2)	4479(24)	−628(11)	9982(25)	55(4)
C(21)	5574(29)	−718(14)	11928(23)	78(7)
C(3)	3211(21)	−1194(10)	8861(21)	50(4)
C(31)	2805(35)	−1988(12)	9394(33)	88(7)
C(4)	2706(24)	−880(11)	7118(22)	56(5)
C(41)	1480(32)	−1357(16)	5434(24)	93(8)
C(5)	3608(21)	−189(10)	7151(21)	50(5)
C(51)	3625(26)	240(11)	5576(21)	65(6)
C(6)	2354(28)	890(12)	10449(22)	62(5)
N(1)	2824(33)	1400(11)	11503(23)	94(6)
C(7)	3414(60)	1983(15)	12778(31)	155(18)
C(8)	3143(49)	2809(16)	12043(47)	168(18)
C(9)	685(27)	−416(12)	10229(24)	61(5)
O(1)	88(25)	−683(11)	11171(20)	94(5)
C(10)	−831(26)	−279(10)	7123(26)	61(5)
O(2)	−2275(19)	−496(11)	6253(20)	88(5)

[a] U_{eq} is defined as one-third of the trace of the orthogonalized U_{ij} tensor.

deposited at the Cambridge Crystallographic Data Centre. Copies of the data can be obtained free of charge on application to The Director, CCDC, 12 Union Road, Cambridge CB2 1EZ, UK (fax: +44 1223 336033; e-mail: teched@Chemcrys.cam.ac.uk).

Acknowledgements

We thank the Fonds der Chemischen Industrie and the Deutsche Forschungsgemeinschaft for financial support, Dr. U. Hartmann and U. Kursawe for the elemental analyses, and Dr. M. von Löwis and A. Woyda for recording the mass spectra.

References

[1] (a) J. Satgé, M. Massol, P. Rivière, J. Organomet. Chem. 56 (1973) 1; (b) P. Rivière, M. Rivière-Baudet, J. Satgé, in: G. Wilkinson, F.G.A. Stone, E.W. Abel (Eds.), Comprehensive Organometallic Chemistry, Vol. 2, Pergamon, Oxford, 1982, p. 399; (c) J. Satgé, Pure Appl. Chem. 56 (1984) 137; (d) W.P. Neumann, Chem. Rev. 91 (1991) 311.

[2] (a) W. Petz, Chem. Rev. 86 (1986) 1019; (b) P. Jutzi, Adv. Organomet. Chem. 26 (1986) 217; (c) M. Veith, Angew. Chem. 99 (1987) 1; Angew. Chem. Int. Ed. Engl. 26 (1987) 1; (d) M.F. Lappert, R.S. Rowe, Coord. Chem. Rev. 100 (1990) 267; (e) M. Driess, H. Grützmacher, Angew. Chem. 108 (1996) 900; Angew. Chem. Int. Ed. Engl. 35 (1996) 828.

[3] (a) D.H. Harris, M.F. Lappert, J. Chem. Soc. Chem. Commun. (1974) 895; (b) P.J. Davidson, D.H. Harris, M.F. Lappert, J. Chem. Soc. Dalton Trans. (1976) 2268; (c) M.F. Lappert, M.J. Slade, J.L. Atwood, M.J. Zaworotko, J. Chem. Soc. Chem. Commun. (1980) 621; (d) B. Cetinkaya, I. Gümrükcü, M.F. Lappert, J.L. Atwood, R.D. Rogers, M.J. Zaworotko, J. Am. Chem. Soc. 102 (1980) 2088; (e) T. Fjeldberg, H. Hope, M.F. Lappert, P.P. Power, A.J. Thorne, J. Chem. Soc. Chem. Commun. (1983) 639; (f) P.B. Hitchcock, M.F. Lappert, B.J. Samways, E.L. Weinberg, ibid. (1983) 1492; (g) T. Fjeldberg, P.B. Hitchcock, M.F. Lappert, S.J. Smith, A.J. Thomas, ibid. (1985) 939; (h) A. Meller, C.-P Gräbe, Chem. Ber. 118 (1985) 2020; (i) T. Fjeldberg, A. Haaland, B.E.R. Schilling, M.F. Lappert, A.J. Thorne, J. Chem. Soc. Dalton Trans. (1986) 1551; (j) P. Jutzi, A. Becker, H.G. Stammler, B. Neumann, Organometallics, 10 (1991) 1647; (k) W.A. Herrmann, M. Denk, J. Behm, W. Scherer, F.-R. Klingan, H. Bock, B. Solouki, M. Wagner, Angew. Chem. 104 (1992) 1489; Angew. Chem. Int. Ed. Engl. 31 (1992) 1485; (l) A.J. Arduengo III, H. Bock, H. Chen, M. Denk, D.A. Dixon, J.C. Green, W.A. Herrmann, N.L. Jones, M. Wagner, R. West, J. Am. Chem. Soc. 116 (1994) 6641; (m) C. Heinemann, W.A. Herrmann, W. Thiel, J. Organomet. Chem. 475 (1994) 73; (n) C. Böhme, G. Frenking, J. Am. Chem. Soc. 118 (1996) 2039.

[4] (a) A.N. Nesmeyanov, K.N. Anisimov, N.E. Kolobova, F.S. Denisov, Izv. Akad. Nauk. SSSR Ser. Khim. (1966) 2246; (b) N. Flitcroft, D.A. Harbourne, I. Paul, P.M. Tucker, F.G.A. Stone, J. Chem. Soc. A (1966) 1130; (c) D.J. Patmore, W.A.G. Graham, Inorg. Chem. 5 (1966) 1405; (d) A.N. Nesmeyanov, K.N. Anisimov, N.E. Kolobova, F.S. Denisov, Izv. Akad. Nauk. SSSR, Ser. Khim. (1968) 142; (e) A.N. Nesmeyanov, K.N. Anisimov, N.E. Kolobova, F.S. Denisov, ibid. (1969) 1520; (f) A.N. Nesmeyanov, L.G. Makarova, V.N. Vinogradova, ibid. (1972) 1449; (g) H. Brunner, S. Loskot, Z. Naturforsch. 28b (1973) 314.

[5] (a) T.S. Piper, G. Wilkinson, J. Inorg. Nucl. Chem. 3 (1956) 104; (b) E.O. Fischer, K. Fichtel, Chem. Ber. 94 (1961) 1200; (c) R.B. King, F.G.A. Stone, Inorg. Synth. 7 (1963) 107; (d) E.O. Fischer, R.L. Pruett, Inorg. Synth. 7 (1963) 136; (e) N.W. Hoffman, Inorg. Chim. Acta 88 (1984) 59; (f) M.J. Morris, in: E.W. Abel, F.G.A. Stone, G. Wilkinson (Eds.), Comprehensive Organometallic Chemistry, Vol. 5, 1995, pp. 404–407.

[6] S.R. Birdwhistell, P. Hackett, A.R. Manning, J. Organomet. Chem. 157 (1978) 239.

[7] (a) M.S. Wrighton, J. Am. Chem. Soc. 97 (1975) 4246; (b) D.C. Miller, R.J. Angelici, J. Organomet. Chem. 394 (1990) 235.

[8] A.N. Nesmeyanov, K.N. Anisimov, N.E. Kolobova, M.Ya. Zakharova, Izv. Akad. Nauk. SSSR Ser. Khim. (1967) 1880.

[9] (a) C.W. Moulton, J.G. Miller, J. Am. Chem. Soc. 78 (1956) 2702; (b) O.M. Nefedov, S.P. Kolesnikov, W.I. Schejtschenko, Angew. Chem. 76 (1964) 498; Angew. Chem. Int. Ed. Engl. 3 (1964) 508; (c) O.M. Nefedov, M.N. Manakov, Angew. Chem. 78 (1966) 1039; Angew. Chem. Int. Ed. Engl. 5 (1966) 1021.

[10] T.J. Marks, A.M. Seyam, Inorg. Chem. 13 (1974) 1624.

[11] J.V. Scibelli, M.D. Curtis, Synth. React. Inorg. Met.-Org. Chem. 8 (1978) 399.

[12] (a) H.R.H. Patil, W.A.G. Graham, Inorg. Chem. 5 (1966) 1401; (b) A. Carrick, F. Glockling, J. Chem. Soc. A (1968) 913.

[13] D.J. Cardin, S.A. Keppie, M.F. Lappert, J. Chem. Soc. A (1970) 2594.

[14] S.A. Keppie, M.F. Lappert, J. Chem. Soc. A (1971) 3216.

[15] L.-P. Lorenz, Gruppentheorie und Molekülsymmetrie, Attempto Verlag, 1992.

[16] (a) L.J. Todd, J.R. Wilkinson, J. Organomet. Chem. 77 (1974) 1; (b) B. Lungwitz, A.C. Filippou, 498 (1995) 91, and references cited therein.

[17] (a) F.C. Wilson, D.P. Shoemaker, J. Chem. Phys. 37 (1957) 809; (b) M.J. Bennett, R. Mason, Proc. Chem. Soc. (1963) 273;

(c) M.R. Churchill, J.P. Fennessey, Inorg. Chem. 6 (1967) 1213; (d) J.E. O'Connor, E.R. Corey, J. Am. Chem. Soc. 89 (1967) 3930; (e) J.B. Wilford, H.M. Powell, J. Chem. Soc. A (1969) 8; (f) J. Rajaram, J.A. Ibers, Inorg. Chem. 12 (1973) 1313; (g) J. St. Denis, W. Butler, M.D. Glick, J.P. Oliver, J. Am. Chem. Soc. 96 (1974) 5427; (h) A.J. Conway, P.B. Hitchcock, J.D. Smith, J. Chem. Soc. Dalton Trans. (1975) 1945; (i) D.E. Crotty, E.R. Corey, T.J. Anderson, M.D. Glick, J.P. Oliver, Inorg. Chem. 16 (1977) 920; (j) M.M. Mickiewicz, C.L. Raston, A.H. White, S.B. Wild, Aust. J. Chem. 30 (1977) 1685; (k) J.N. St. Denis, W. Butler, M.D. Glick, J.P. Oliver, J. Organomet. Chem. 129 (1977) 1; (l) P. Leoni, E. Grilli, M. Pasquali, M. Tomassini, J. Chem. Soc. Dalton Trans. (1986) 1041.

[18] C. Bueno, M.R. Churchill, Inorg. Chem. 20 (1981) 2197.

[19] L.Y.Y. Chan, W.K. Dean, W.A.G. Graham, Inorg. Chem. 16 (1977) 1067.

[20] F. Carré, E. Colomer, R.J.P. Corriu, A. Vioux, Organometallics 3 (1984) 970.

[21] R.S. Simons, P.P. Power, J. Am. Chem. Soc. 118 (1996) 11966.

[22] L.K. Figge, P.J. Carroll, D.H. Berry, Organometallics 15 (1996) 209.

[23] Y. Morino, Y. Nakamura, T. Iijima, J. Chem. Phys. 32 (1960) 643.

[24] P. Venkateswarlu, R.C. Mockler, W. Gordy, J. Chem. Phys. 21 (1953) 1713.

[25] J.E. Drake, J.L. Hencher, Q. Shen, Can. J. Chem. 55 (1977) 1104.

[26] L. Fajari, L. Julia, J. Riera, E. Molins, C. Miravitlles, J. Organomet. Chem. 363 (1989) 31.

[27] J.E. Drake, R.T. Hemmings, J.L. Hencher, F.M. Mustoe, Q. Shen, J. Chem. Soc. Dalton Trans. (1976) 394, and references cited therein.

[28] A.C. Filippou, J.G. Winter, G. Kociok-Köhn, I. Hinz, unpublished results.

[29] (a) A.R. Manning, J. Chem. Soc. A (1967) 1984; (b) R.B. King, R.H. Reimann, D.J. Darensbourg, J. Organomet. Chem. 93 (1975) C23; (c) D.L. Beach, K.W. Barnett, ibid. 97 (1975) C27; (d) D.L. Beach, M. Dattilo, K.W. Barnett, ibid. 140 (1977) 47; (e) R.B. King, R.H. Reimann, Inorg. Chem. 15 (1976) 183.

[30] U. Schubert, K. Ackermann, R. Janta, S. Voran, W. Malisch, Chem. Ber. 115 (1982) 2003.

[31] L.J. Todd, J.R. Wilkinson, J.P. Hickey, D.L. Beach, K.W. Barnett, J. Organomet. Chem. 154 (1978) 151.

[32] E.O. Fischer, E. Moser, J. Organomet. Chem. 5 (1966) 63.

[33] (a) R.B. King, Inorg. Chem. 2 (1963) 936; (b) E.O. Fischer, E. Moser, J. Organomet. Chem. 2 (1964) 230; (c) P.M. Treichel, K.W. Barnett, R.L. Shubkin, ibid. 7 (1967) 449; (d) K.W. Barnett, D.W. Slocum, ibid. 44 (1972) 1; (e) R.B. King, J. Gimeno, Inorg. Chem. 17 (1978) 2396; (f) D.J. Blumer, K.W. Barnett, T.L. Brown, J. Organomet. Chem. 173 (1979) 71; (g) J. Febvay, F. Casabianca, J.G. Riess, Inorg. Chem. 24 (1985) 3235; (h) K. Stärker, M.D. Curtis, ibid. 24 (1985) 3006.

[34] (a) M.R. Churchill, J.P. Fennessey, Inorg. Chem. 7 (1968) 953; (b) J.H. Cross, R.H. Fenn, J. Chem. Soc. A (1970) 3019; (c) M.T. McPhail, G.R. Knox, C.G. Robertson, G.A. Sim, J. Chem. Soc. A (1971) 205; (d) A.G.U. Hardy, G.A. Sim, J. Chem. Soc. Dalton Trans. (1972) 1900; (e) R.D. Adams, D.F. Chodosh, Inorg. Chem. 17 (1978) 41; (f) G.M. Reisner, I. Bernal, H. Brunner, M. Muschiol, B. Siebrecht, J. Chem. Soc. Chem. Commun. (1978) 691.

[35] (a) A.C. Filippou, W. Grünleitner, Z. Naturforsch. 44b (1989) 1572; (b) A.C. Filippou, E.O. Fischer, W. Grünleitner, J. Organomet. Chem. 386 (1990) 333; (c) A.C. Filippou, W. Grünleitner, ibid. 407 (1991) 61; (d) A.C. Filippou, W. Grünleitner, E.O. Fischer, ibid. 411 (1991) C21.

[36] (a) A.C. Filippou, W. Grünleitner, P. Kiprof, J. Organomet. Chem. 410 (1991) 175; (b) A.C. Filippou, W. Grünleitner, C. Völkl, P. Kiprof, ibid. 413 (1991) 181; (c) A.C. Filippou, C. Völk, P. Kiprof, ibid. 415 (1991) 375; (d) A.C. Filippou, C. Völkl, R.D. Rogers, ibid. 463 (1993) 135; (e) A.C. Filippou, B. Lungwitz, C. Völkl, E. Herdtweck, ibid. 502 (1995) 131.

[37] D.J. Cronin, J.R. Wilkinson, L.J. Todd, J. Magn. Res. 17 (1975) 353.

[38] (a) S.P. Kolesnikov, I.S. Rogozhin, O.M. Nefedov, Izv. Akad. Nauk. SSSR Ser. Khim. 10 (1974) 2379; S.P. Kolesnikov, I.S. Rogozhin, O.M. Nefedov, Chem. Abstr. 82 (1975) 25328 u.

[39] H.J. Lucas, E.R. Kennedy, Org. Synth. Collect. Vol. 3 (1976) 482.

[40] M.L. Lütkens, Jr., A.P. Sattelberger, H.H. Murray, J.D. Basil, J.P. Fackler, Jr., Inorg. Synth. 26 (1989) 7; W. Wolfsberger, H. Schmidbaur, Synth. React. Inorg. Met. Org. Chem. 4 (1974) 149.

[41] (a) J. Casanova, Jr., R.E. Schuster, N.D. Werner, J. Chem. Soc. (1963) 4280; (b) R.E. Schuster, J.E. Scott, J. Casanova, Jr., Org. Synth. 46 (1966) 75.

[42] J. Pickardt, UTILITY, Technische Universität Berlin, Germany, 1994.

[43] G.M. Sheldrick, SHELXS-86, Program for Crystal Structure Solution, Universität Göttingen, Germany, 1986.

[44] G.M. Sheldrick, SHELXL-93, Program for Crystal Structure Determination, Universität Göttingen, Germany, 1993.

[45] D.T. Cromer, J.B. Mann, Acta Crystallogr. A 24 (1968) 321.

[46] (a) A.L. Spek, PLUTON-92, PLATON-93, graphics program, University of Utrecht, Netherlands, 1992 and 1993; (b.) A.L. Spek, Acta Crystallogr. A, 46 (1990) C34.

[47] L. Zsolnai, H. Pritzkow, ZORTEP, ORTEP program for PC, Universität Heidelberg, 1994.

[48] H.D. Flack, Acta Crystallogr. A 39 (1983) 876.